

Formation and propagation of shield-like precipitation pattern in the Eastern China Sea remotely enhanced by Typhoon Nepartak (2016) simulated by an atmosphere-wave-ocean coupled model

Akiyoshi Wada^{1*}, Hiroshige Tsuguti¹ and Hiroyuki Yamada²

¹Meteorological Research Institute, Tsukuba, Ibaraki, 305-0052, JAPAN

²University of the Ryukyus, 1 Senbaru, Nishihara-cho, Nakagami-gun, Okinawa, 903-0213, JAPAN
*awada@mri-jma.go.jp

1. Introduction

Typhoon Nepartak was the first tropical cyclone in the typhoon season of 2016. The storm induced distant rainbands that propagated northward toward the Amami Islands. Wada et al. (2017) reported that the behavior of the rainbands and resultant shield-like precipitation pattern were reasonably simulated by a nonhydrostatic atmosphere model (NHM) and an atmosphere-wave-ocean coupled model (CPL) (Wada et al., 2010).

During the west northwestward translation of Nepartak, distant rainbands induced by the typhoon propagated toward the Amami Islands. The rainbands formed a shield-like precipitation pattern in the Eastern China Sea (Fig. 1). Then the precipitation pattern formed a low pressure area that caused heavy rainfalls in the southern part of Kyusyu (Fig. 2). This report focuses on formation and propagation of the shield-like precipitation pattern in the Eastern China Sea enhanced by the storm.

2. Experimental design

Numerical simulations were conducted by the NHM and CPL, respectively. The experimental design was almost the same as Wada et al. (2017) except that the standard longitude was set to 130° E. It covered a 4140 km x 4140 km area with a horizontal grid spacing of 3 km. The integration time was 120 hours with the time steps of 3 seconds in the NHM, 18seconds in the ocean model and 10 minutes in the ocean wave model. The initial time was 1800 UTC on 4 July in 2016. NHM had 55 vertical levels with variable intervals from 40 m for the near-surface layer to 1013 m for the uppermost layer. The top height was ~26 km. The simulations used the Japan Meteorological Agency global objective analysis data for atmospheric initial and boundary conditions (with a horizontal grid spacing of ~20km) and the daily oceanic reanalysis data calculated by the Meteorological Research Institute multivariate ocean variational estimation (MOVE) system (Usui et al. 2006) with a horizontal grid spacing of 0.5°. The inhibition rate of evaporation of rain, snow and graupel was set to 0.7. This report will show the results simulated by the CPL.

3. Results

3.1 Track and central pressure simulations

Figure 3 shows results of track and central pressure simulations for 120 hours started from 1800 UTC on 4 July. The track was reasonable simulated by the NHM and CPL. However, rapid intensification of the storm from 4 to 6 July could not be simulated by the NHM and CPL. The central pressure simulated by the NHM reached the minimum (~894 hPa) at 1330 UTC 7 July, which was later than the best track central pressure did.

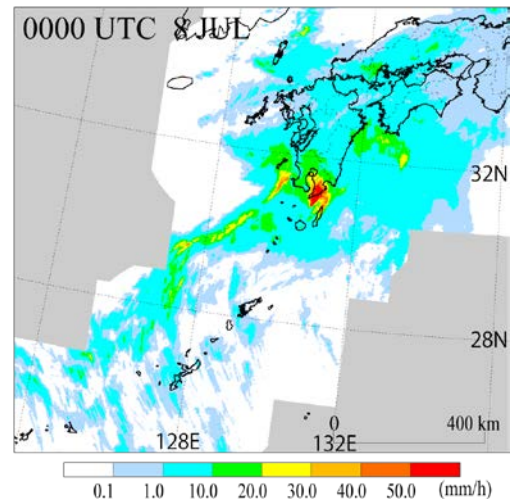


Figure 1. Horizontal distribution of the Radar-Raingauge analyzed hourly precipitation amount at 0000 UTC on 8 July in 2017.

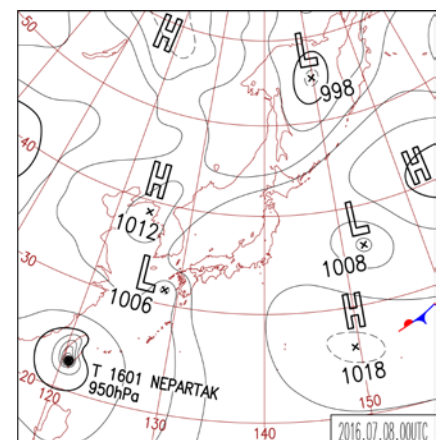


Figure 2. Weather map at 0000 UTC 8 July in 2016.

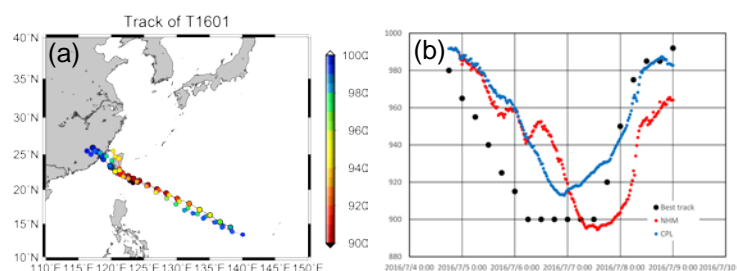


Figure 3 Results of (a) track simulations and best track location of Nepartak with colors indicating the value of central pressure and (b) time series of simulated central pressure with best-track central pressure. Red indicates the results simulated by the NHM. Blue indicates the results simulated by the CPL. Black indicates the best track data.

3.2 Formation and propagation of shield-like precipitation pattern

Figure 4 shows the horizontal distributions of hourly precipitation simulated by the CPL. At 0600UTC on 7 July, a shield-like precipitation pattern was reasonably simulated. The shield-like precipitation area was formed by distant rainbands propagated from the storm that moved northwestward toward Taiwan Main Island (Fig. 4a). The hourly precipitation within the shield-like precipitation area locally increased in the East China Sea at 0000 UTC on 8 July (Fig. 4b). Although the shield-like precipitation area was better simulated than that reported in Wada et al. (2017), the location of the area still differed from that obtained from the Radar-Raingauge analyzed hourly precipitation amount (Fig. 1). Note that the location of the shield-like precipitation pattern simulated by the NHM was different from the location simulated by the CPL. This suggests that ocean coupling could affect the propagation of distant rainband and formation of the shield-like precipitation pattern.

Figure 5 shows the time series of hourly precipitation simulated by the CPL. The rainband propagated about 500 km for 12 hours, indicating that the moving speed was approximately 11.5 m s^{-1} . Ran and Chen (2016) reported the generation of inertial-gravity waves in a severe convective system occurred in East China. The moving speed was estimated to be approximately 13.9 m s^{-1} according to their Fig. 4d, which is consistent with the moving speed of the rainband propagation. The propagation was terminated at around 1800 UTC on July. The shield-like precipitation area then moved eastward along 30°N while developing as an extratropical cyclone.

In order to validate the simulation results shown in Fig. 5, Global Satellite Mapping of Precipitation (GSMaP) dataset (<http://sharaku.eorc.jaxa.jp/GSMaP/index.htm>) was used. Figure 6 shows the time series of hourly precipitation obtained from GSMaP data. GSMaP data represents the propagation of the rainfall areas, the termination of the propagation at around 30°N , and eastward movement along 30°N while developing as an extratropical cyclone. The result provides the evidence that the results simulated by the CPL were reasonable to examine the formation and propagation processes of shield-like precipitation pattern.

4. Concluding remarks

This simulation result is considered to be a remote effect induced by a storm different from the Predecessor Rain Event (PRE: e.g., Galarneau et al., 2010) in that the location of the shield-like rainfall pattern was not “ahead”. The area of high total water content was simulated at around 6–8 km altitude in the shield-like precipitation area and moved along with the propagation of the shield-like precipitation area. Understanding how this propagation process was realized is important for understanding the formation process of the shield-like precipitation area.

References

- Galarneau, T., J., L. F. Bosart and R. S. Schumacher (2010). Predecessor rain event ahead of tropical cyclones. *Mon. Weather Rev.*, 138, 3272–3297.
 Ran, L. and C. Chen (2016). Diagnosis of the forcing of inertial-gravity waves in a severe convective system. *Adv. Atmos. Sci.*, 33, 1271–1284.
 Wada, A., N. Kohno and Y. Kawai (2010). Impact of wave-ocean interaction on Typhoon Hai-Tang in 2005. *SOLA*, 6A, 13–16.
 Wada, A., H. Tsuguti and H. Yamada: Numerical simulations of shield-like precipitation pattern in the Eastern China Sea remotely enhanced by Typhoon Nepartak (2016). *CAS/JSC WGNE Res. Activities in Atm. And. Oceanic Modelling*. 47, 5–24.

Acknowledgement

This work was supported by JSPS KAKENHI Grant Number JP16H04053 and JP15K05292.

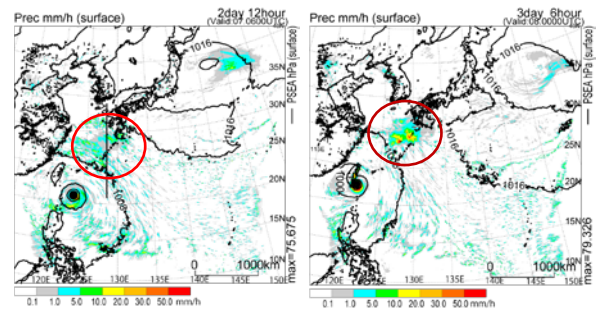


Figure 4 Horizontal distributions of hourly precipitation (shades) with sea-level pressures (contours) simulated by the CPL (a) at 0600 UTC on 7 July and (b) at 0000 UTC on 8 July. Contour intervals are 8 hPa. The line in (a) indicates the location of cross section.

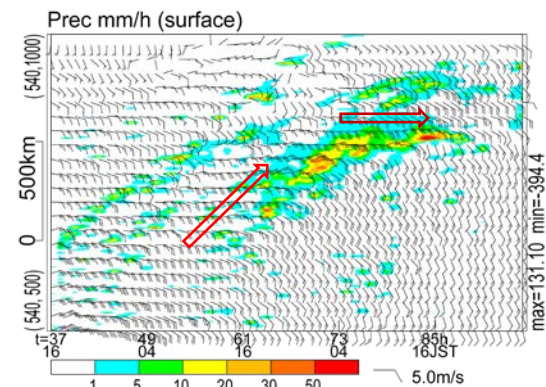


Figure 5 Time series of hourly precipitation (shades) with 20-m wind vectors (whether wind symbols) simulated by the CPL. The vertical axis corresponds to the line shown in Fig. 4.

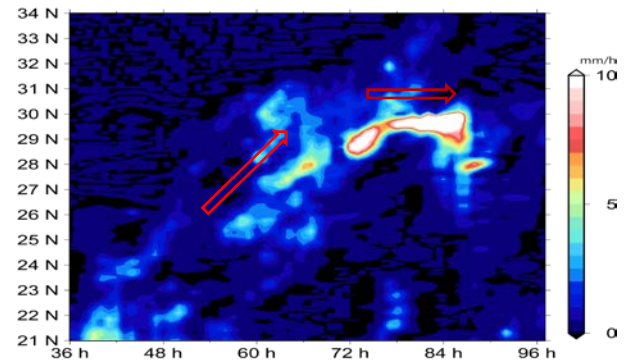


Figure 6 Same as Fig. 5 except that GSMaP was used for drawing the time series.